Nano Energy 31 (2017) 560–567

Contents lists available at ScienceDirect

Nano Energy

journal homepage: www.elsevier.com/locate/nanoen

Spring-assisted triboelectric nanogenerator for efficiently harvesting water wave energy

Tao Jiang[a,1], Yanyan Yao[a,1], Liang Xu[a], Limin Zhang[a], Tianxiao Xiao[a], Zhong Lin Wang[a,b,*]

[a] Beijing Institute of Nanoenergy and Nanosystems, Chinese Academy of Sciences; National Center for Nanoscience and Technology (NCNST), Beijing 100083, China

[b] School of Materials Science and Engineering, Georgia Institute of Technology, Atlanta, GA 30332-0245, USA

ARTICLE INFO

Keywords:
Triboelectric nanogenerator
Spring-assisted
Water wave energy
Blue energy

ABSTRACT

Ocean waves are one of the most promising renewable energy sources for large-scope applications. Triboelectric nanogenerator (TENG) has been demonstrated to effectively harvest water wave energy possibly toward large-scale blue energy. In this work, a kind of spring-assisted TENG was designed and investigated for harvesting water wave energy. The idea of introducing spring is to store the potential energy built during mechanical triggering for multiple cycles of conversion into electricity afterward, and transform a low frequency motion into a high frequency oscillation for improving the energy harvesting efficiency. The output performance of the basic unit was optimized by adjusting the motor acceleration and spring parameters including the rigidity and length. There exists an optimized spring rigidity or spring length to produce the highest performance. By using the spring, the accumulated charge of the TENG can be increased by 113.0%, and the translated electric energy or efficiency can be improved by 150.3%. Then four optimized basic units were connected in parallel and packaged into a sealed box to harvest the water wave energy. The present work could provide an approach to improving the output performance and efficiency of TENGs in harvesting low-frequency water wave energy.

1. Introduction

Due to the increasing threat of fuel shortage and energy crisis, scavenging new energy sources from our natural environment has attracted considerable interests [1,2]. Water wave, wind, and solar energies are all clean and renewable energy sources with great potential for large-scope applications, in which the water wave energy from the ocean exhibits superior advantages over other energy sources with a much less dependence on season, day or night, weather, and temperature conditions [3,4]. Nevertheless, harvesting such widely distributed water energy is rather challenging due to various limitations of current technologies [5,6]. So far, the converters for harvesting the water wave energy to generate electricity are mostly based on the electromagnetic generators, which are heavy, bulky, costly, easily corroded, and inefficient at ocean wave frequency [7–9]. The serious challenges and situations drive us to make efforts to seek a lightweight, small-sized, cost-effective, and highly-efficient approach for harvesting the water wave energy.

Recently, triboelectric nanogenerator (TENG) has emerged as a powerful technology for harvesting mechanical energy, with advantages of high output power, high efficiency, low fabrication cost, and no pollution [10–16]. The TENG can convert mechanical energy from a variety of sources to electricity through the coupling effect of contact electrification and electrostatic induction [17–20]. Our previous work indicated that TENG has a much better performance than that of electromagnetic generator at low frequency (typically 0.1–3 Hz), which verifies the possible killer application of a TENG for harvesting low frequency energy from motions such as ocean waves [21]. The TENG has been demonstrated to effectively harvest water wave energy in previously published works and possess huge potential toward large-scale blue energy harvesting from the ocean [22–29]. However, these TENG devices for water wave energy harvesting are all confronted with a problem that the TENGs move and work simultaneously with the water waves, and they are nearly at the same motion frequency. Because of the very low frequency of water waves, the harvested wave energy and translated electric energy at a certain short time are very limited. If a deformable component (such as a spring) is applied in the TENG device to store the mechanical energy under the water wave impact, the energy harvested from the water waves, containing the kinetic energy of TENG motional component and stored elastic

* Corresponding author at: Beijing Institute of Nanoenergy and Nanosystems, Chinese Academy of Sciences; National Center for Nanoscience and Technology (NCNST), Beijing 100083, China.
E-mail address: zlwang@gatech.edu (Z.L. Wang).
[1] These authors contribute equally to this work.

http://dx.doi.org/10.1016/j.nanoen.2016.12.004
Received 5 November 2016; Received in revised form 29 November 2016; Accepted 4 December 2016
Available online 06 December 2016

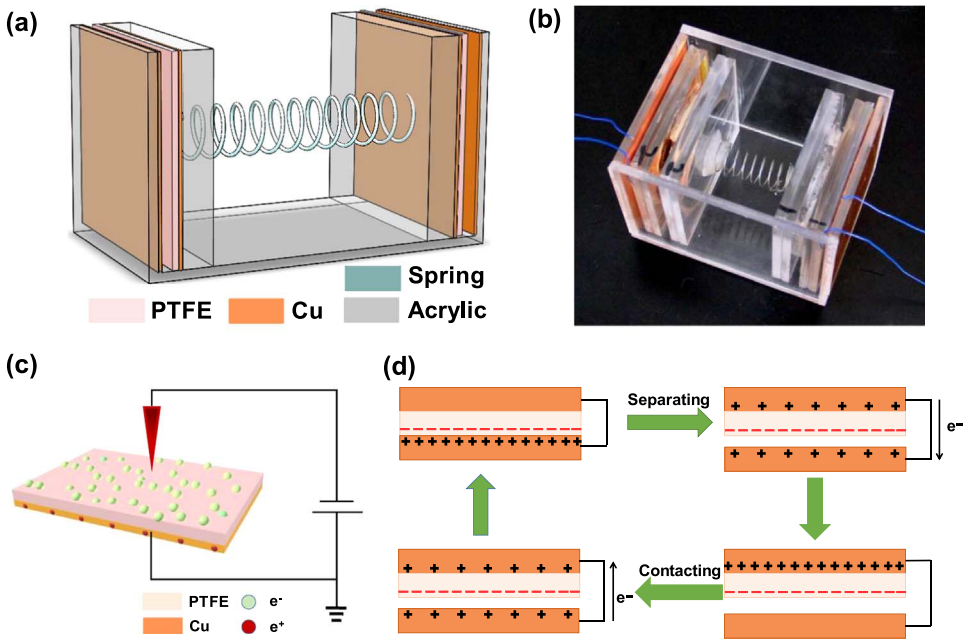

Fig. 1. (a) Schematic illustration of the spring-assisted TENG structure. (b) Photograph of the fabricated spring-assisted TENG device. (c) Schematic the electron injection process for generating negative charges on the surface of PTFE. (d) Working principle of the spring-assisted TENG device.

potential energy, can be increased due to the continuous oscillations after the mechanical triggering. The elastic potential can further act on the motional component, possibly translating the low frequency motion into a high frequency motion and longer-period of motion, and enhance the energy conversion efficiency.

In the present work, we designed a kind of spring-assisted TENG for harvesting water wave energy, in which two Cu-PTFE-covered acrylic blocks connected by a spring are placed between two Cu electrodes anchored on two internal walls of the box-like device. This TENG structure based on the contact-separation between PTFE films and Cu electrodes can serve as a basic unit of the TENG network. First, the output performance of the basic unit was measured under the regular action of linear motor. The influences of motor acceleration, spring rigidity, and spring length were investigated, and the TENG was structurally optimized by adjusting the spring parameters. Then, we connected four optimized basic units in parallel and packaged them into a sealed box to harvest the water wave energy. Finally, under the action of water waves, the unit number dependent output behavior was revealed, and the integrated TENG device was utilized to charge a capacitor. The work provides the strategies for improving the output performance and efficiency of TENGs in harvesting water wave energy.

2. Experimental section

2.1. Fabrication of the spring-assisted TENGs

First, two 80 μm thick PTFE films were deposited with a layer of copper on one side as the electrode. The copper sides of two Cu-PTFE films were tightly attached to two acrylic blocks with a size of 7 cm×7 cm. By placing a needle above the PTFE surface of Cu-PTFE film with a height of 5 mm, connecting the needle to the cathode, and connecting the Cu electrode to the anode and ground, electrons were injected to the top surface of FEP film. A polarization voltage of 5 kV was applied for 5 min. Second, a circular iron with a diameter of 5.5 cm was sandwiched between an acrylic block bonded with Cu-PTFE film and another pristine acrylic block to increase the total mass. Two whole acrylic blocks (embed by irons) were connected by a spring with a moderate rigidity and a length of about 4.5 cm. Third, a open acrylic box with an outside dimension of 10.5 cm×8.5 cm×8.0 cm was fabricated, and its inside has the space of 9.5 cm×7.5 cm×7.5 cm to hold the spring-connected acrylic blocks. Two Cu electrodes were anchored on two internal walls of the box, and some lubricant oils were sprayed on the bottom internal surface of the acrylic box to facilitate the sliding friction. Based on the contact electrification between PTFE films on acrylic blocks and Cu electrodes on the internal walls, the spring-assisted TENG device was finally obtained. In the experiments, we chose three kinds of springs with different rigidities. For the rigid, moderate, and flexible springs, the compression rates are respectively 1.0 kg cm^{-1}, 0.2 kg cm^{-1}, and 0.1 kg cm^{-1}, and the maximum loads are 2.5 kg, 0.7 kg, and 0.4 kg, respectively.

For the water wave harvesting, four spring-assisted TENG units with a moderate spring rigidity were fabricated. They are placed into the reserved space of a pre-prepared acrylic box with an outside dimension of 21.5 cm×21.5 cm×8.5 cm. The spring length was chosen as 4.5 cm, and the four reserved spaces all have the size of 9.5 cm×7.5 cm×7.5 cm, which are large enough to hold the TENG units. The four spring-assisted TENG units contained eight TENGs, and each TENG was connected to a rectifier bridge, and then they were electrically connected in parallel. The acrylic box was finally sealed and waterproofing was processed.

2.2. Electrical measurement of the TENGs

The output voltage and current signals of the devices were measured by a digital oscilloscope (Agilent InfiniiVision 2000X) and a current preamplifier (Keithley 6514 System Electrometer).

3. Results and discussion

A kind of spring-assisted TENG was designed and fabricated, as schematically shown in Fig. 1a. The TENG device is composed of two parts: an acrylic box and two spring-connected acrylic blocks. The acrylic box is used to hold the spring-connected acrylic blocks. On two internal walls of the box, there are two Cu electrodes anchored. The surfaces of the two acrylic blocks are tightly attached by the copper sides of two Cu-PTFE films. The detailed fabrication process of the TENG device can be found in the Experimental section. A photograph of an as-fabricated TENG device is shown in Fig. 1b. To increase the total mass of the acrylic blocks, which can increase contact force and improve the contact completeness, a small circular iron is embed into

either acrylic block. In the experiments, an iron was used to be sandwiched between an acrylic block bonded with Cu-PTFE film and another pristine acrylic block, as shown in Fig. 1b.

To increase the surface charge of PTFE and improve the output performances of TENG, electrons were first injected to the top surface of PTFE film with Cu electrode on its backside, using the method published in the literatures [30–32]. Fig. 1c shows the schematic process of the electron injection on the PTFE surface. The needle was connected to the cathode and the Cu electrode was connected to the anode and ground, then the needle point was directly faced to the PTFE surface with a vertical distance of 5 mm. When a polarization voltage of 5 kV was applied on the needle lasting for 5 min, numerous electrons were injected from the needle point to the PTFE film surface, and the bottom electrode under the PTFE film was induced with positive charges from the ground to screen the electrical field during this process. In addition, the working principle of the spring-assisted TENG is similar to common contact-separation mode TENG, which is schematically shown in Fig. 1d. Under an external triggering, such as the water wave impact, the PTFE layers on the surfaces of acrylic blocks collide and contact with the Cu electrodes on box walls, generating positive triboelectric charges on the Cu and negative ones on the PTFE surface. Due to the periodic character of external triggering (*e.g.*, water wave impact), the PTFE layer and Cu then separate and produce an inner dipole moment between the two contact surfaces. That drives free electrons from the Cu electrode on the backside of PTFE to the bottom Cu electrode to balance the electric field, producing positively induced charges on the top Cu electrode. The electron flow lasts until the maximum separation. When the two surfaces get close to each other again until complete contact, free electrons flow back to the top Cu electrode on PTFE, forming a complete cycle of electricity generation process.

We first fabricated a spring-assisted TENG device by using a spring with moderate rigidity and a length L of 4.5 cm. The spring rigidity should be appropriate so that the elastic force of the spring can be comparable to the mass force of acrylic blocks, and then the acrylic blocks can slide freely on the bottom surface of the acrylic box. The typical electrical output results of the spring-assisted TENG device under the regular action of linear motor are presented in Fig. 2. The maximum displacement of the motor, *i.e.*, maximum displacement of external box, was fixed as 9.0 cm. The maximum reached speed and acceleration of the motor are 1 m s^{-1} and 5 m s^{-2}, respectively. Note that in one spring-assisted TENG device there are two TENGs and thereby only the results of one TENG are shown. Under the currently adopted conditions, the output voltage, current, and transferred charge can arrive at 458.3 V, 45.8 μA, and 162.1 nC, as respectively shown in Fig. 2a-c. We can also clearly view the peak character of these output signals from Fig. 2a-c and enlarged plots of voltage, current, and charge during one cycle as shown in Fig. S1 of Supporting information. The voltage exhibits two large positive peaks, two large negative peaks, and several small peaks. The large peaks indicate there are two electricity-generating cycles during one cycle of linear motor, because the motor stayed for 0.2 s at both ends of the motion displacement. The appearance of these small peaks can be attributed to the action of the spring. Similar to the voltage, there exist multiple small peaks in the current profile. The spring with stored elastic potential energy can further push or drag the acrylic blocks, leading to the horizontal vibration of acrylic blocks. This phenomenon, similar to that in the literature [33], can be clearly reflected by the up-down fluctuation of the transferred charge (Fig. 2c, Fig. S1c). During one cycle of linear motor, the motional acrylic blocks exhibit multiple cycles although some cycles are not complete, and in contrast with the low frequency of linear motor, the motion frequency of acrylic blocks is relatively higher. Therefore, the elastic spring can translate the low frequency motion into a high frequency motion, and the spring-assisted TENG structure may play an important role in the water wave energy harvesting. For the current motor conditions, the TENG can transit an instantaneous power of 5.38 mW at the matched resistance of 10 MΩ (Fig. 2d). In addition, the frequency-dependent output behavior for the spring-assisted TENG was also studied. The motor did not stay at both ends of the motion displacement, and the motor acceleration was changed to reflect different motion frequencies, whose values can be extracted from the output signals. The peak value of the transferred charge with respect to the frequency is shown in Fig. S2. The transferred charge can reach the maximum at the moderate frequency, and the resonant frequency of this TENG device is about 4.75 Hz. The decrease of charge at a higher frequency can be ascribed to the hindered of collision

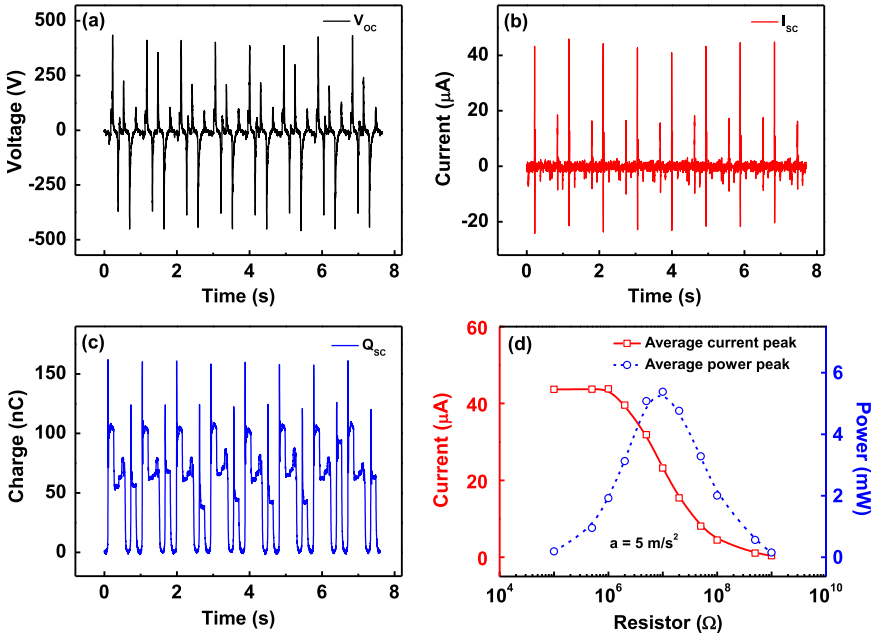

Fig. 2. Electric output of the spring-assisted TENG device under the action of linear motor: (a) output voltage; (b) output current; (c) transferred charge; (d) average current peak and average power peak as functions of the resistance. The maximum speed and acceleration of the motor are 1 m s^{-1} and 5 m s^{-2}.

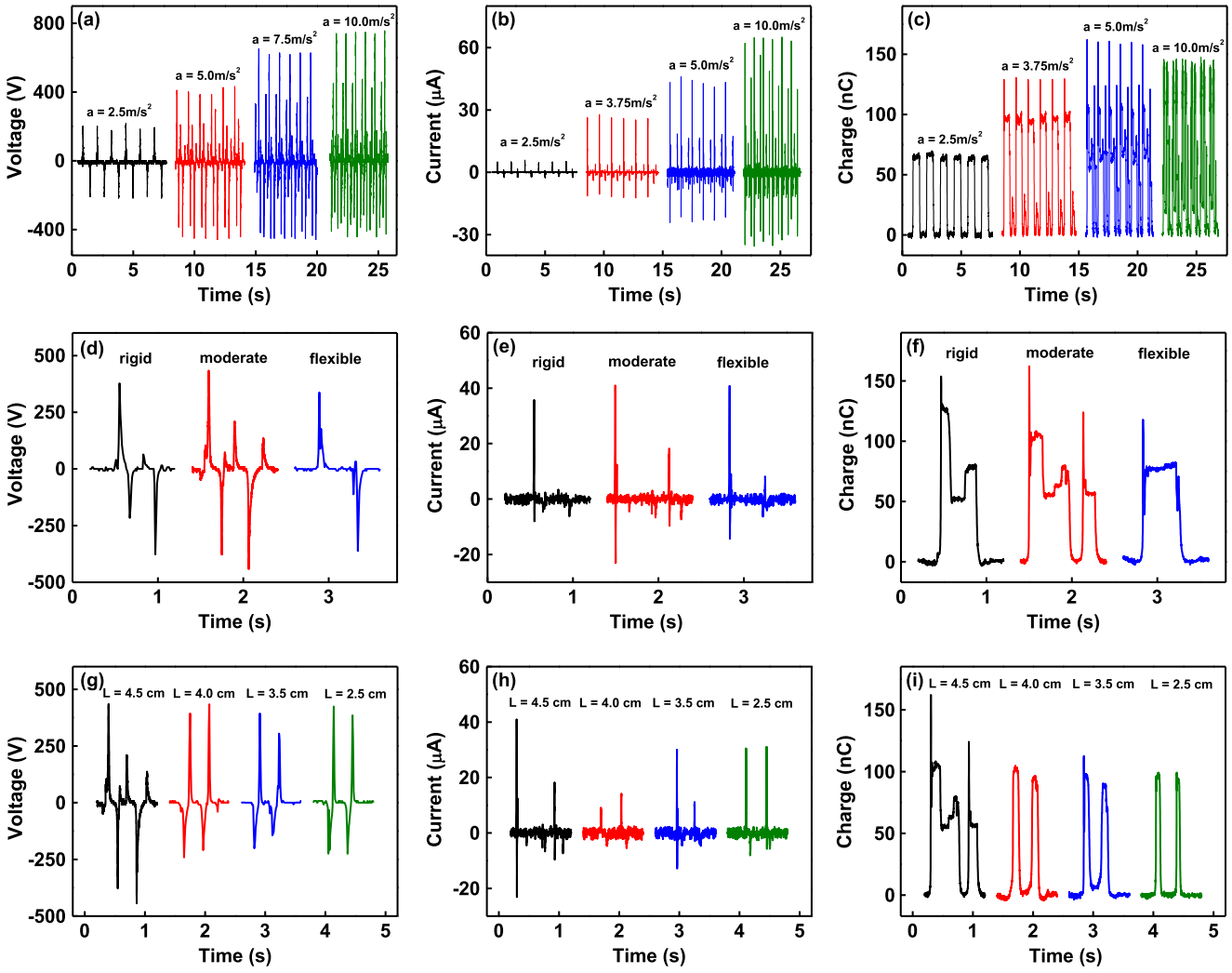

Fig. 3. (a-c) Effects of the motor acceleration on (a) output voltage; (b) output current; (c) transferred charge of the spring-assisted TENG. The maximum speed of the motor is 1 m s^{-1}. (d-f) Effects of the spring rigidity on (d) output voltage; (e) output current; (f) transferred charge. The maximum speed and acceleration of the motor are 1 m s^{-1} and 5 m s^{-2}. (g-i) Effects of spring length on (g) output voltage; (h) output current; (i) transferred charge.

between the acrylic blocks and box wall by the strong drag force of the spring at the higher frequency.

To deepen the understanding of the output behavior for the spring-assisted TENG, the influences of the motor acceleration and spring parameters including the rigidity and length on the electric output were investigated. The output voltage, current, and charge for the TENG as functions of the motor acceleration a are shown in Fig. 3a-c. It can be seen that as the acceleration of the motor increases from 2.5 m s^{-2} to 10 m s^{-2}, the peak values of voltage and current both increase. The voltage and current can respectively reach 755.8 V and 65.0 μA at a=10 m s^{-2}. The peak value of transferred charge first increases and then slightly decreases at a higher acceleration. The drop of the charge is because that the strong drag force of the spring at the higher acceleration hinders slightly the collision between the acrylic blocks and box wall. To show the moving path of the TENG at different motor accelerations, a video was taken and provided as Video S1. Based on the observed moving path, we can explain the effect of the motor acceleration on the output performance. Besides the peak values of output signals, the acceleration also affects the profile shape of voltage, current, and charge. For example, at a lower acceleration (2.5 m s^{-2}), the voltage and current have only one positive peak and only one negative peak in one cycle, and the charge has a plateau value. That implies the action of spring is tiny at the lower acceleration. The contribution of the spring increases with increasing the motor acceleration, which can be also viewed from the profile character of charge (Fig. 3c).

Supplementary material related to this article can be found online at doi:10.1016/j.nanoen.2016.12.004.

The effects of the spring rigidity on the output voltage, current, and transferred charge were then studied and shown in Fig. 3d-f. The maximum speed and acceleration of the motor were set to be 1 m s^{-1} and 5 m s^{-2}. The complete output profiles for rigid and flexible springs are shown in Fig. S3. For the spring-assisted TENG with a very rigid spring, the voltage exhibits two positive peaks and two negative peaks in one cycle, lack of multiple small peaks like the moderate spring rigidity. The current shows a large positive peak and two small negative peaks, resulting from the two increases and two decreases of transferred charge. The horizontal vibration of acrylic blocks cannot be observed in this situation, indicating that the two acrylic blocks together with the spring can be considered as an entire rigid body. Relative to the moderate spring rigidity, the decreased motion velocity of the rigid body will lead to lower voltage and current peaks. The spring cannot take effect in translating low frequency into high frequency. On the other hand, the electric outputs for the TENG with a flexible spring are also different. The voltage possesses one positive peak and one negative peak, but the current exhibits two positive peaks

and two negative peaks. The charge is much lower than that of larger spring rigidity, ascribed to the weaker elastic force in the flexible spring. The spring cannot push or drag the acrylic blocks to get extra electric output peaks. Therefore, a moderate spring rigidity is necessary for the spring-assisted TENG to produce higher output performance and more electric energy.

Fig. 3g-i shows the voltage, current, and charge results of TENG for various spring lengths L. The length of spring varies from 4.5 to 2.5 cm, and the complete profiles of voltage, current, and charge for various spring lengths are presented in Fig. S4. As can be seen, when the spring length decreases from 4.5 cm, the small peaks resulting from the action of spring in the voltage profile disappear, and the voltage exhibits two positive peaks and two negative peaks in the spring length range from 4.0 to 2.5 cm (Fig. 3g). The maximum current decreases due to the great decrease of transferred charge (Fig. 3h and i), and previous multiple small peaks in current profile also disappear. The vibrations of acrylic blocks and spring do not exist, because a shorter spring is more difficult to be stretched and compressed, especially at L=2.5 cm the acrylic blocks together with the spring become a rigid body. The acrylic blocks connected by a shorter spring with larger moving space cannot collide with the box walls completely, so the transferred charge is largely decreased. Note that the TENG with L=4.0 cm has a very low current which is ascribed to the cooperative action of the larger moving space and lower moving velocity (higher spring force). From the above analysis, we can find that a larger spring length within the allowable range is preferred for the spring to take effect.

To quantitatively analyze the improvement of the output performance for the TENG by using the elastic spring, we fabricated a similar TENG device by just displacing the spring by a solid acrylic strip. We measured the electric properties of the TENG without the spring, and the load characteristic indicates the TENG can transit an instantaneous power of 4.89 mW at the matched load of 10 MΩ, as shown in Fig. S5. By comparing the output voltage and current for these two TENGs, we find the spring-assisted TENG can exhibit higher average peak values of voltage and current than the TENG without a spring. The voltage can be increased by 22.8%, and the current can be increased by 29.6%. Then the accumulated charge was measured as plotted in Fig. 4a. It is obvious that in contrast with the TENG with acrylic strip, the accumulated charge realized by the spring-assisted TENG in one cycle can be enhanced from 351.03 nC to 747.84 nC (by 113.0%), because of more conversion cycles under the action of spring. Then the resistive load characteristics of the two TENGs were also compared. Fig. 4b shows the current profiles of the TENGs in one cycle at the matched load resistance of 10 MΩ. For the spring-assisted TENG, we can clearly observe the multiple cycles of high frequency oscillation, but for the TENG without the spring, the oscillation does not appear ascribed to the constraint of rigid acrylic strip. Through the time integration of the instantaneous power on the load resistance, we can calculate the generated electric energy on the load, whose equation is given by

$$E_{out} = \int I^2 R dt \tag{1}$$

About ten cycles for the current-time curve at a load resistor were chosen to calculate the total electric energy. Then we can obtain the average electric energy in one cycle. The electric energy of the two TENGs in one cycle was calculated for various resistances and shown in Fig. 4c. As can be seen, the electric energy reaches the maximum values at the resistance of 10 MΩ for both the two TENGs. The electric energy produced by using the spring can be improved by up to 150.3%. That is because the spring stores the potential energy built during mechanical triggering for multiple cycles of conversion into electricity afterward. For the energy conversion efficiency, we can calculate it by the ratio of output electric energy to the input mechanical energy, using the formula

$$\eta = \frac{E_{out}}{E_{in}} \times 100\% = \frac{\int I^2 R dt}{E_{in}} \times 100\% \tag{2}$$

where the input energy E_{in} is difficult to be determined in such systems, but the input energies are the same for the TENGs with the spring and without the spring, therefore, the energy conversion efficiency can also be improved by 150.3% when using the spring.

To demonstrate the application of spring-assisted TENG in water wave energy harvesting, four optimized basic spring-assisted TENG units were integrated into the reserved space of a pre-prepared acrylic box, as the photograph shows in Fig. 5a. Each of the eight TENGs in the four spring-assisted TENG units is connected to a rectifier bridge and then electrically connected in parallel. The acrylic box was finally sealed and waterproofing was processed. The fabrication details are described in the Experimental section. A photo of sealed device floating on water in a pool connected with scores of LEDs is shown in Fig. 5b. Triggered by the water wave motion, these LEDs can be lightened up (see the inset). A video named as Video S2 was also captured to demonstrate the capacity of the device to harvest water wave energy. The rectified output voltage and current of the spring-assisted TENGs were measured as shown in Fig. 5c and d. Similar to our previous work [25], the seesawing motion of the tank with water inside at fixed amplitude and frequency will generate the water waves for experimental measurement. It can be found that the peak values of the voltage and current are 562.8 V and 71.8 μA, respectively. Enlarged views of output for the device with four units in Fig. S6 show the multi-peak character of voltage signal and current signal, because the motion of each unit can not be synchronous absolutely, and also there exists the action of the spring. The small peaks generated by the spring vibration are superimposed over the peaks from the nonsynchronous motion of TENG units, which can be reflected by the 12 peaks appearing on the current profile in a short time of 0.1 s (see Fig. S6c). Then we measured the

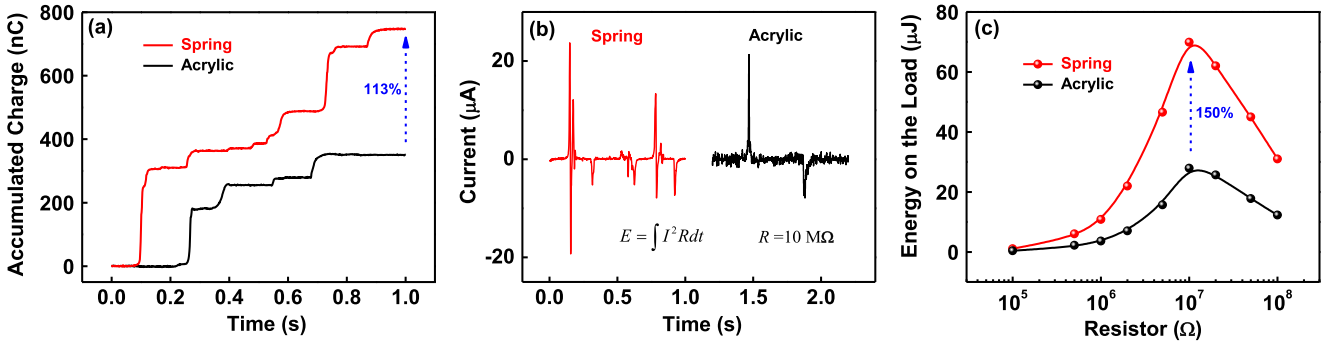

Fig. 4. Comparison of the output performances for the TENGs with spring and without spring (the spring is displaced by an acrylic strip). (a) Accumulated charge of the TENGs in one cycle. (b) Output current of two TENGs in one cycle at the matched load resistance of 10 MΩ. (c) Translated electric energy on the load in one cycle as a function of the load resistance for two TENGs.

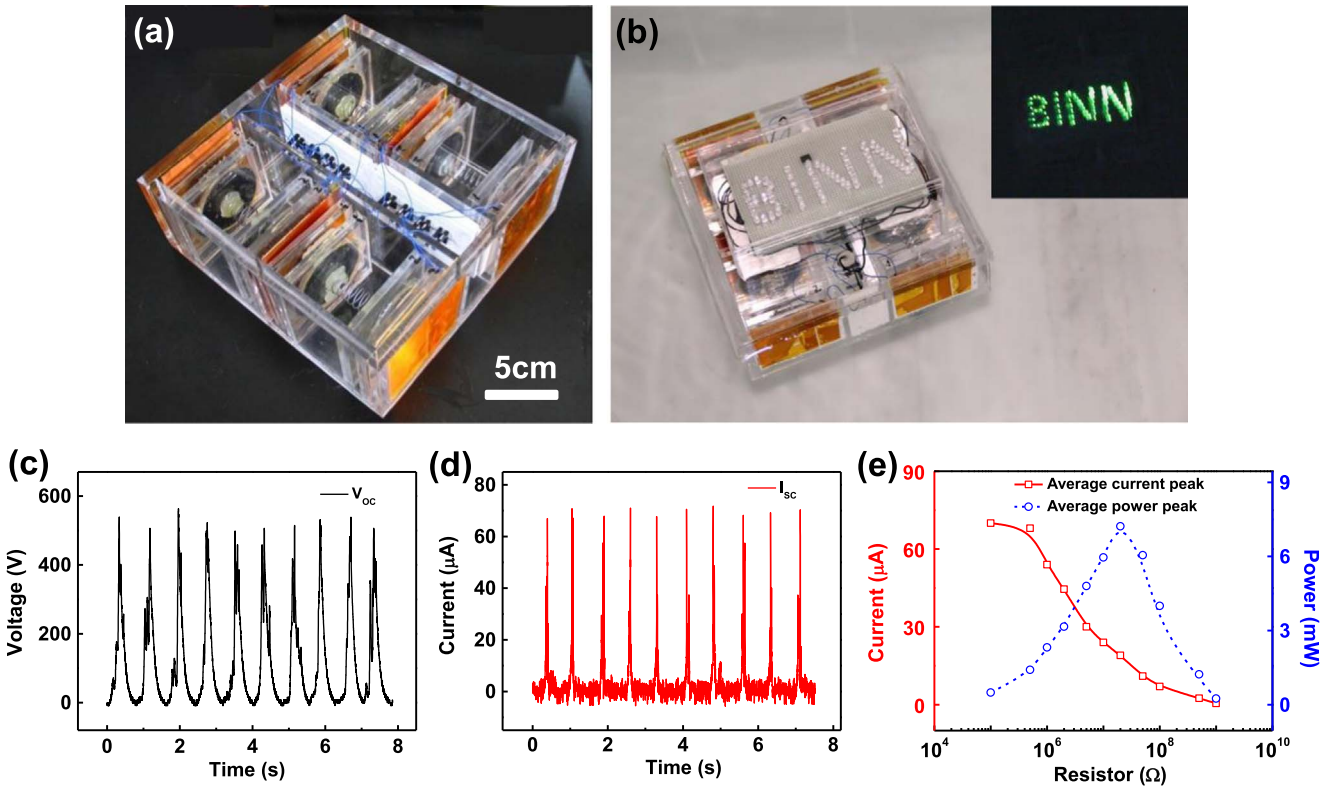

Fig. 5. (a) Device structure of spring-assisted TENGs for harvesting water wave energy. (b) Photograph of the device floating on water and optical images of 70 LEDs driven by the water wave. (c) Output voltage and (d) output current of the device under the simple wave condition. (e) Average current peak and average power peak as functions of the resistance for the integrated device.

resistive load behavior of the integrated device, and found the device can produce an instantaneous peak power of 7.22 mW at the matched resistance of 20 MΩ, as shown in Fig. 5e. According to the volume of the box device (99.38 cm^3), we can obtain the maximum power density of 726.48 mW/m^3. Note that to simulate the real ocean water environment, we are adding enough salts into the water of the pool. We are making the mass density of the water close to that of the seawater. In the present work, the corrosion of acrylic box by the seawater is not considered. However, in the further investigations, the corrosion issue and life time of the TENG device will be addressed

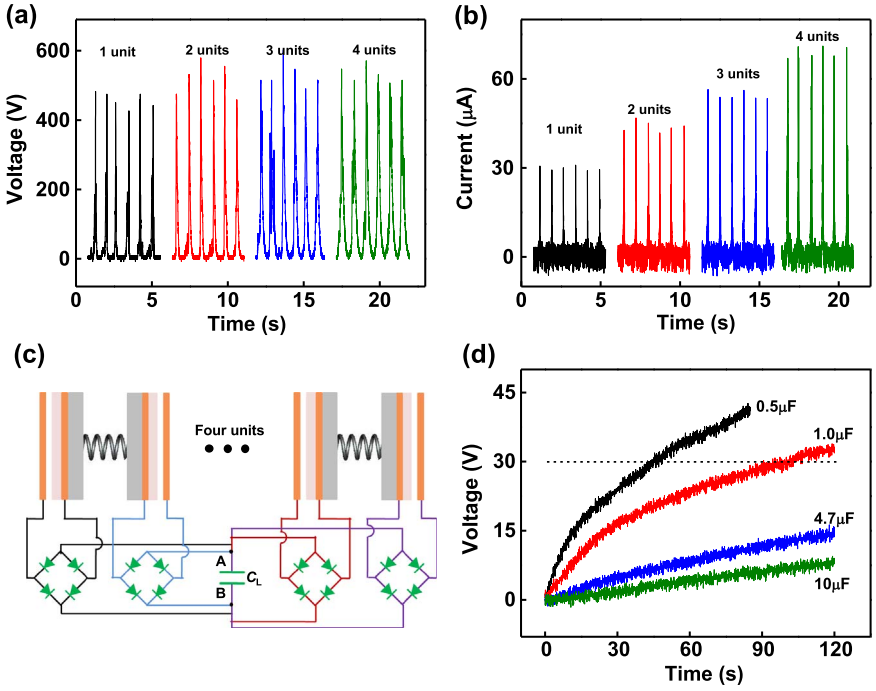

Fig. 6. (a-b) Effect of the unit number on the electric output: (a) output voltage; (b) output current. (c) Schematic diagram of utilizing the TENG device with four parallel spring-assisted units to charge a capacitor. (d) Charging voltage as a function of the charging time for various capacitances.

carefully.

Supplementary material related to this article can be found online at doi:10.1016/j.nanoen.2016.12.004.

The effect of unit number on the output performance of the intergrated TENGs was also examined and the output voltage and current of the spring-assisted TENGs with unit number n=1, 2, 3, 4 were respectively presented in Fig. 6a and b. As can be seen, with increasing the unit number, the average voltage peak amplitudes almost hold constant, although the peak density of voltage signal increases. That is because of the electrically parallel connection between each TENG unit. For the current output, the amplitudes of current peaks increase markedly with increasing the unit number, and the peak density of current signal also increases. From Fig. 6b, we can see the average current amplitude at n=1 is about 29.6 μA, and it is greatly increased to 70.2 μA at n=4. For further extension, if thousands of such units are integrated and work together as the TENG network, the large-scope blue energy will be effectively harvested. In real applications, the harvested energy needs to be stored by an energy storage unit such as capacitor or battery, providing a regulated and manageable output, because the uncontrollable and unstable nature of environmental water waves leads to unstable converted electrical energy from TENGs, which cannot be directly used to power electronic devices. Fig. 6c shows the schematic illustration of utilizing the TENG device with four parallel spring-assisted units to charge a capacitor. The charging voltages on various load capacitances as a function of the charging time were measured by a voltage meter (Keithley 6514 System electrometer) and shown in Fig. 6d. The charging voltage is higher for a smaller load capacitance and charging speed is faster. The integrated spring-assisted TENG device can charge a 1 μF capacitor to 30 V in about 100 s, and the output charge without external load reaches 30 μC. Of course, for more efficient energy harvesting and storage, an integrated system including the electricity-generating, rectification, management, storage, and transmission should be developed and applied in the water wave energy harvesting.

4. Conclusions

In summary, we have designed and fabricated a kind of spring-assisted TENG for harvesting water wave energy, which has a box structure composed of two Cu-PTFE-covered acrylic blocks connected by a spring and two Cu electrodes anchored on two internal walls of the box. The output performance of the basic unit was measured under the regular action of linear motor, and the influences of motor acceleration, spring rigidity, and spring length were investigated. The results indicate that there exists an optimized spring rigidity or spring length for the spring-assisted TENG to reach the highest outputs. The spring can store the elastic potential energy and further act on the TENG, leading to the appearance of multiple small peaks in the voltage/current signal and the up-down fluctuation of transferred charge. By using the spring, the accumulated charge of the TENG can be increased by 113.0%, and the translated electric energy or efficiency can be improved by 150.3%. Then the as-fabricated TENG device with four spring-assisted TENG units has been demonstrated to successfully harvest the water wave energy, producing high output dependent on the unit number. This work could provide useful information for the spring-assisted TENGs in the applications of efficiently harvesting water wave energy.

Acknowledgements

Supports from the “thousands talents” program for the pioneer researcher and his innovation team, the National Key R & D Project from Minister of Science and Technology (2016YFA0202704), National Natural Science Foundation of China (Grant No. 51432005, 5151101243, and 51561145021), and Project funded by China Postdoctoral Science Foundation (2016M590070) are appreciated. Patents have been filed based on the research results presented in this manuscript.

Appendix A. Supplementary material

Supplementary data associated with this article can be found in the online version at doi:10.1016/j.nanoen.2016.12.004.

References

[1] J.P. Painuly, Renew. Energy 24 (2001) 73–89.
[2] A. Khaligh, O.C. Onar, Energy Harvesting: Solar, Wind, and Ocean Energy Conversion Systems, CRC Press, Boca Raton, FL, 2009.
[3] A.F. de, O. Falcao, Renew. Sust. Energy Rev. 14 (2010) 899–918.
[4] Z.L. Wang, J. Chen, L. Lin, Energy Environ. Sci. 8 (2015) 2250–2282.
[5] S.H. Salter, Nature 249 (1974) 720–724.
[6] J. Falnes, Mar. Struct. 20 (2007) 185–201.
[7] A.V. Jouanne, Mech. Eng. Mag. 128 (2006) 24–27.
[8] R. Henderson, Renew. Energy 31 (2006) 271–283.
[9] A. Wolfbrandt, IEEE Trans. Magn. 42 (2007) 1812–1819.
[10] F.R. Fan, Z.Q. Tian, Z.L. Wang, Nano Energy 1 (2012) 328–334.
[11] G. Zhu, Y.S. Zhou, P. Bai, X.S. Meng, Q. Jing, J. Chen, Z.L. Wang, Adv. Mater. 26 (2014) 3788–3796.
[12] T. Jiang, X. Chen, C.B. Han, W. Tang, Z.L. Wang, Adv. Funct. Mater. 25 (2015) 2928–2938.
[13] S.H. Wang, L. Lin, Z.L. Wang, Nano Energy 11 (2015) 436–462.
[14] Y.N. Xie, S.H. Wang, S.M. Niu, L. Lin, Q.S. Jing, J. Yang, Z.Y. Wu, Z.L. Wang, Adv. Mater. 26 (2014) 6599–6607.
[15] L. Lin, Y.N. Xie, S.M. Niu, S.H. Wang, P.-K. Yang, Z.L. Wang, ACS Nano 9 (2015) 922–930.
[16] W. Tang, T. Jiang, F.R. Fan, A.F. Yu, C. Zhang, X. Cao, Z.L. Wang, Adv. Funct. Mater. 25 (2015) 3718–3725.
[17] C.B. Han, W.M. Du, C. Zhang, W. Tang, L.M. Zhang, Z.L. Wang, Nano Energy 6 (2014) 59–65.
[18] T. Jiang, W. Tang, X. Chen, C.B. Han, L. Lin, Y. Zi, Z.L. Wang, Z. L. Adv. Mater. Technol. 1 (2016) 1600017.
[19] T. Jiang, X. Chen, K. Yang, C.B. Han, W. Tang, Z.L. Wang, Nano Res. 9 (2016) 1057–1070.
[20] X. Chen, T. Jiang, Y. Yao, L. Xu, Z. Zhao, Z.L. Wang, Adv. Funct. Mater. 26 (2016) 4906–4913.
[21] Y. Zi, H. Guo, Z. Wen, M.-H. Yeh, C. Hu, Z.L. Wang, ACS Nano 10 (2016) 4797–4805.
[22] Y.J. Su, X.N. Wen, G. Zhu, J. Yang, J. Chen, P. Bai, Z.M. Wu, Y.D. Jiang, Z.L. Wang, Nano Energy 9 (2014) 186–195.
[23] G. Zhu, Y.J. Su, P. Bai, J. Chen, Q.S. Jing, W.Q. Yang, Z.L. Wang, ACS Nano 8 (2014) 6031–6037.
[24] J. Chen, J. Yang, Z.L. Li, X. Fan, Y.L. Zi, Q.S. Jing, H.Y. Guo, Z. Wen, K.C. Pradel, S.M. Niu, Z.L. Wang, ACS Nano 9 (2015) 3324–3331.
[25] T. Jiang, L.M. Zhang, X.Y. Chen, C.B. Han, W. Tang, C. Zhang, L. Xu, Z.L. Wang, ACS Nano 9 (2015) 12562–12572.
[26] L. Zhang, C.B. Han, T. Jiang, T. Zhou, X. Li, C. Zhang, Z.L. Wang, Nano Energy 22 (2016) 87–94.
[27] X.F. Wang, S.M. Niu, Y.J. Yin, F. Yi, Z. You, Z.L. Wang, Adv. Energy Mater. 5 (2015) 1501467.
[28] Y. Yao, T. Jiang, L. Zhang, X. Chen, Z. Gao, Z.L. Wang, ACS Appl. Mater. Interfaces 8 (2016) 21398–21406.
[29] Z. Wen, H. Guo, Y. Zi, M.-H. Yeh, X. Wang, J. Deng, J. Wang, S. Li, C. Hu, L. Zhu, Z.L. Wang, ACS Nano 10 (2016) 6526–6534.
[30] S.H. Wang, Y.N. Xie, S.M. Niu, L. Lin, C. Liu, Y.S. Zhou, Z.L. Wang, Adv. Mater. 26 (2014) 6720–6728.
[31] M. Eguchi, Philos. Mag. 49 (1925) 178–192.
[32] T. Zhou, L. Zhang, F. Xue, W. Tang, C. Zhang, Z.L. Wang, Nano Res. 9 (2016) 1442–1451.
[33] M. Ma, Q. Liao, G. Zhang, Z. Zhang, Q. Liang, Y. Zhang, Adv. Funct. Mater. 25 (2015) 6489–6494.

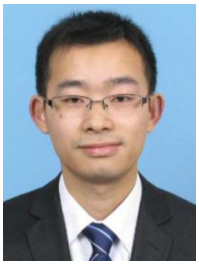

Dr. **Tao Jiang** received his Ph.D. degree from East China University of Science and Technology in 2014. Now he is an associate researcher in Prof. Zhong Lin (Z.L.) Wang's group at the Beijing Institute of Nanoenergy and Nanosystems, Chinese Academy of Sciences. His research interests are the theoretical studies of triboelectric nanogenerators, and practical applications in self-powered sensing and blue energy harvesting.

Yanyan Yao received her undergraduate degree from Shandong University in 2013, and her major is Materials Science and Engineering, and now she is a graduate student in Beijing Institute of Nanoenergy and Nanosystems, Chinese Academy of Sciences. Her research interests are focused on blue energy harvesting by using triboelectric nanogenerator.

Dr. **Liang Xu** received his Ph.D. degree from Tsinghua University (THU) in 2012, with awards of Excellent Doctoral Dissertation of THU and Excellent Graduate of Beijing. Before that he achieved bachelor's degree of mechanical engineering in Huazhong University of Science & Technology (HUST) in 2007. He is now a postdoctoral fellow in Beijing Institute of Nanoenergy and Nanosystems, Chinese Academy of Sciences (CAS), under the supervision of Prof. Zhong Lin Wang. His research interests include nanogenerators and self-powered nanosystems, fundamental tribological phenomena, scanning probe microscopy and molecular dynamics simulation.

Limin Zhang received her undergraduate degree from Hebei University of Technology in 2012, and now she is a doctoral candidate. Her research interests are piezoelectric nanogenerator and triboelectric nanogenerator, especially focus on triboelectricity based active micro/nano-sensors, flexible electronics, tribotronic circuit and their applications in sensor networks and human machine interaction.

Tianxiao Xiao received his undergraduate degree from Dalian University of Technology in 2015, and his major is Polymer Materials and Engineering, and now he is a graduate student in Beijing Institute of Nanoenergy and Nanosystems, Chinese Academy of Sciences. Her research interests are focused on the optimization of the blue energy harvesting systems.

Prof. **Zhong Lin Wang** received his Ph.D from Arizona State University in physics. He now is the Hightower Chair in Materials Science and Engineering, Regents' Professor, Engineering Distinguished Professor and Director, Center for Nanostructure Characterization, at Georgia Tech. Dr. Wang has made original and innovative contributions to the synthesis, discovery, characterization and understanding of fundamental physical properties of oxide nanobelts and nanowires, as well as applications of nanowires in energy sciences, electronics, optoelectronics and biological science. His discovery and breakthroughs in developing nanogenerators established the principle and technological road map for harvesting mechanical energy from environment and biological systems for powering a personal electronics. His research on self-powered nanosystems has inspired the worldwide effort in academia and industry for studying energy for micro-nano-systems, which is now a distinct disciplinary in energy research and future sensor networks. He coined and pioneered the field of piezotronics and piezo-phototronics by introducing piezoelectric potential gated charge transport process in fabricating new electronic and optoelectronic devices. Details can be found at: www.nanoscience.gatech.edu.